

PhytClub - A Novel siRNA Formulation for the Biocontrol of Pepper Foot Rot

Akshay Arun Prasath, Shivam Mohite, Ankith Suhas Rao, Meena Cindamani, Arya Binu, Tanvi Rege, Varun Chacko, Chaithanya Padmar, Ananya BS, V Sai Pallavi, Sanvi Gupta, Shreya Ghosh, Amogh Thale, Harshini Musuvathi Kishore Kumar, Neha Sahajwani, Keena Ravi, Armaan Gupta, Aditi Rishiraj

Team MIT-MAHE, Manipal Institute of Technology, India

Abstract— Pepper foot rot caused by *Phytophthora capsici* severely impacts black pepper production. This study presents a targeted RNAi strategy that uses siRNA targeting the *bZIP1* gene, combined with chitosan nanoparticles to enhance the stability, delivery, and uptake of the siRNA by the pathogen.

I. INTRODUCTION

Piper nigrum L., commonly known as black pepper, is a high-value spice crop grown predominantly in India, Vietnam, Ethiopia, Malaysia, and Indonesia [1]–[3]. Its cultivation is severely threatened by pepper foot rot, a condition caused by the oomycete *Phytophthora capsici*. The infection causes leaf necrosis, rapid drooping, and eventual death within days. Over 561,500 tonnes of pepper is grown each year across 26 countries. In India, Kerala loses up to 1000 tonnes annually [4], and on the West Coast, vine mortality is about 9.64%, costing \$900/ha and up to \$1838/ha in extreme cases [5]. Globally, Vietnam cultivates 131,000 ha as of 2020 and saw a 10,000 ha decline in 2016 due to 95% infection [1]. Ethiopia reported 95% vine infection [2]; Indonesia and Malaysia lost up to 40% and 10% yields, respectively [3]. The mode of infection through zoospores and appressorium formation makes *P. capsici* particularly difficult to curb [6]. Current biocontrol measures are ineffective and cause significant environmental harm.

RNA interference (RNAi) has emerged as an effective strategy for controlling plant pathogens. Small interfering RNA (siRNA) utilises this mechanism to degrade complementary mRNA, enabling the targeted silencing of pathogenic genes. However, the practical application of siRNA is limited by its instability, poor cellular uptake, and degradation in soil. Chitosan nanoparticles offer a promising solution due to their ability to efficiently encapsulate and deliver siRNA.

This study combines therapeutics and nanobiotechnology with computational optimization to develop and evaluate a chitosan-based siRNA nanoformulation against *P. capsici*. The study focuses on the *bZIP1* transcription factor, which regulates

appressorium formation, zoospore motility, and cyst germination [7]. The experimentation involves synthesising the nanoformulation and assessing its effectiveness. A novel software pipeline was developed using Selenium and Machine Learning to help researchers build gene silencing systems easily. This integrated approach aims to establish a sustainable, targeted biocontrol measure to manage pepper foot rot.

II. MATERIALS AND METHODS

A. Selection of Gene of Interest

An extensive literature review demonstrated that *bZIP1* from *Phytophthora infestans* regulates key infection processes, including zoospore motility, cyst germination, appressorium formation, and host invasion. Most importantly, silencing this gene results in complete infection failure despite normal hyphal and sporangial development [7],[8].

On referring to transcriptomic data on *Phytophthora capsici*, the transcription factor *bZIP1* (Protein ID: 128162) was identified. This gene is highly upregulated during early infection ($\text{Log}_2\text{FC}: 6.86, \text{padj} = 6.51\text{E}-12$) [9].

B. Design of siRNA

An extensive literature review confirmed the expression of *bZIP1* at various stages of disease [9].

The nucleotide sequence and transcript for *bZIP1* were obtained from the JGI PhycoCosm database [8],[10].

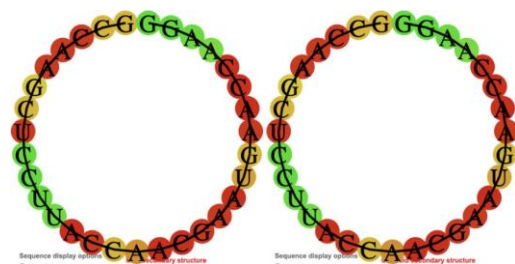


Fig. 1. Secondary structure prediction of the candidate two siRNA target site with flanking regions in the mRNA using RNAfold.

Once the *bZIP* transcript had been retrieved, possible siRNA candidates were predicted using siRNAPred and siDirect [11].

The top-ranking results were subsequently refined using parameters selected through consultation with experts. These included seed-region stability, GC content, thermodynamic profiles, self-complementarity checks, and off-target minimisation.

Secondary structure predictions (Figs. 1 and 3) were conducted to validate the efficacy of the selected candidates. DuplexFold was used to assess the stability of siRNA duplexes, while RNAfold was employed to evaluate the accessibility of the target mRNA region [12]-[14].

Such analysis enabled the assessment of silencing efficiency by ensuring that the guide strands could bind to accessible regions of the mRNA and form energetically favourable duplexes. The inclusion of these computational checks is strongly supported by the literature [15].

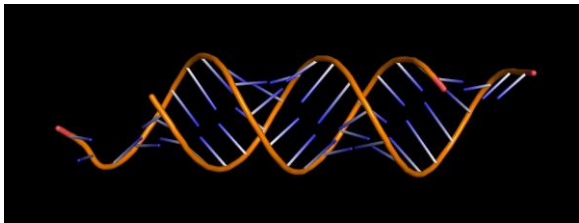


Fig. 2. siRNA duplex of candidate one generated using RNAComposer and visualised in PyMOL.

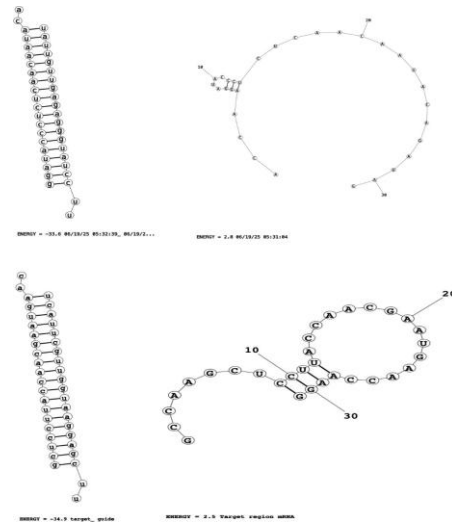


Fig. 3. DuplexFold and MaxExpect results for siRNA candidates 1 and 2 respectively.

TABLE I. THE FINALISED SIRNA CANDIDATES ALONG WITH THEIR PROPERTIES

No.	Sense Strand	Antisense Strand	Target site	Guide seed low GC	Guide 10-14 low GC	Guide 18/19 = G/C	Sense 1-5 high GC	Sense 10 = U	Sense 13 ≠ G	Sense 19/20 = A	Guide strand hairpin	MaxExpect Energy	DuplexFold Energy
1	5' --ggauaccucucaac aauaca 3'	3' --uuccuaugggagag uuguuu--5'	166----- -186	6 A/U bases	1 G/C – low GC	18 = C	2 G/C bases	No (C)	Yes (A)	19 = A, 20 = C	NO	2.8	-33.6
2	5' --gcuccuuaccaacga augaac 3'	3' --uucgaggaugguu gcuuacu--5'	142----1 62	3 A/U bases	Moderate GC	18 = G, 19 = C	4 G/C bases	No (A)	Is G	19 = A	NO	2.5	-34.9
3	5' --caaucugcuucguag uuuaga 3'	3' --gaguuaagacgaagca ucaaa--5'	1026--- 1046	5 A/U bases	3 G/C	18 = G	Only 1 C, rest A/U	Yes	Is G	20 = A	NO	2.6	-30.1
4	5' --gucaugcguacagc gaaacu 3'	3'gccaguacagcaugu cgcuuu--5	59----- 79	5 A/U bases	2 G/C	19 = C	2 G/C bases	Yes	Is A	19 = A	NO	2.7	-33.5

C. Chitosan Nanoparticle Synthesis

0.1% (w/v) low-molecular-weight chitosan (Sigma Aldrich, 75-88% deacetylated) was dissolved in 1% (v/v) acetic acid and stirred for 30 minutes. The pH was then adjusted to 4.0 using 1 N NaOH. A 0.24% (w/v) TPP solution was prepared in sterile distilled water. The chitosan

solution was probe-sonicated at 40% amplitude with 10-second pulses for 5 minutes, then filtered, while the TPP solution was syringe-sterilised using a 0.22 µm PVDF filter. 10 mL of TPP was added dropwise (7s between drops) to 30 mL of stirring chitosan. The suspension was stirred for an additional 20 minutes, transferred to a 50 mL Falcon tube and sonicated. It was then centrifuged at 1000 rpm for 5

minutes at room temperature. 20 mL of supernatant was carefully decanted into a fresh tube and characterised using a Particle Size Analyser (Horiba SZ-100).

D. siRNA Encapsulation

All solutions were made RNase-free. A 0.1% (w/v) chitosan solution was stirred for 30 minutes, after which it was sonicated and filtered as done earlier. A 0.24% (w/v) TPP solution was prepared in RNase-free water and sterilised. 15 µL of 100 µM siRNA in nuclease-free water was mixed with 10 mL TPP and added dropwise to 30 mL of chitosan under stirring. The nanoparticle suspension was transferred to a 50 mL Falcon tube, sonicated for 10 minutes, and centrifuged at 1000 rpm for 5 minutes. A 20 mL supernatant was carefully decanted and stored at 4 °C.

E. Gel Retardation Assay and Entrapment Efficiency

The protocol was adapted from Katas & Alpar (2006). 35 mL of 2% agarose gel was prepared using a 1x TBE buffer. 10 µL of the RNA ladder and various samples (nanoparticle solution, encapsulated siRNA, naked siRNA, and encapsulated siRNA treated with 2 µL of 0.5 mg/mL RNase) were loaded onto the gel upon a 1:6 dilution with the loading dye. Electrophoresis was carried out at 55V for 2 hours. The gel was visualised under a UV transilluminator at 365 nm.

The encapsulated siRNA sample was centrifuged at 11,000 rpm for 37 minutes at 4°C. 2 µL of the supernatant was loaded onto a nanocuvette, and its absorbance was measured at 260 nm using a UV-vis spectrophotometer.

The entrapment efficiency was calculated using the formula:

$$\text{Entrapment Efficiency (\%)} = \frac{C_{\text{sample}} - C_{\text{supernatant}}}{C_{\text{sample}}} \times 100$$

Where C_{sample} is the concentration of siRNA added, and $C_{\text{supernatant}}$ is the siRNA concentration in the supernatant [16].

F. Characterisation using Particle Size Analyser and Scanning Electron Microscopy (SEM)

The chitosan nanoparticles and the nanoformulation were analysed using a Particle Size Analyser (Horiba Scientific Nano Partica SZ-100). Approximately 1 to 2 mL was transferred into a clean glass zetasizer cell, ensuring that no air bubbles were present. The zeta potential and hydrodynamic radius measurements were performed at room temperature in triplicate.

Samples were smeared on glass coverlips and gold sputtered to make them conductive for SEM analysis using an Oxford EDS (X-act) scanning electron microscope (fresh samples) and a JEOL FESEM 7610F PLUS (3-week-old samples).

G. *Phytophthora capsici* Culturing and Zoospore Induction

8mm plugs of *Phytophthora capsici* from the parent culture were inoculated onto carrot agar media, with the mycelium facing downwards. Cultures were incubated in the dark at 25°C.

12-15 mycelial plugs were isolated from 72-hour-old cultures and incubated under light for 48 hours at 29°C. Subsequently, the solution was cold-shocked at 4°C for 30 minutes to release zoospores from the sporangiophores. It was visualised using methylene blue staining (1:5 dye-to-sample ratio) at 40x and 100x magnification.

H. Zoospore Motility Assay

On isolating zoospores, 6 µL of the suspension was taken into six RNase-free PCR tubes. 4 µL of chitosan nanoparticles, 1% acetic acid, 7.23 µM siRNA, 100 µM siRNA, and the nanoformulation were added to five of these tubes, leaving one to serve as the negative control. These samples were incubated for 30 minutes and stained with methylene blue. They were mounted on glass slides and observed at 10x, 40x, and 100x magnification using an Olympus CX-43 upright trinocular phase-contrast microscope.

I. Detached Leaf Assay (DLA)

Equally mature leaves of *Piper nigrum* (Panniyur-1 variety) were plucked and cleaned. They were placed in air-tight containers lined with a layer of wet cotton that had been treated under UV. Pin-pricks were made tightly at the centre of the leaf. 10 µL of every control (plain leaf with no holes, leaf with holes alone, leaf with holes and water, acetic acid) and test sample (chitosan nanoparticle solution, naked siRNA, nanoformulation) was applied onto the leaf. The experiment was performed in biological and technical replicates.

A 5mm plug from a 72-hour-old *Phytophthora capsici* culture was placed such that the mycelium faced the leaf. Necrosis was observed over 3 days.

J. Fluorescence Microscopy

To visualise siRNA uptake by *P. capsici* zoospores, the siRNA was labelled with 6-FAM, a fluorophore with excitation and emission wavelengths of 495 nm and 517 nm respectively. Zoospore suspensions were cold shocked, stained, and quantified using a hemocytometer. These were then diluted to the desired concentration. 4 µL of 100 ng/mL siRNA was added to 6 µL of zoospore suspension at 10⁵ spores/mL, resulting in a final concentration of 40 ng/mL. The zoospores were incubated with the naked siRNA, nanoparticles, nanoformulation, and acetic acid for 90 minutes. Samples were mounted on a glass slide and visualised using an Olympus IX73 fluorescence microscope at 10×, 40×, and 60× magnification.

III. RESULTS

A. siRNA Design

A thorough review of siRNA candidates allowed us to identify the most viable duplexes (listed in Table 2 below) for experimental testing.

TABLE II. FINAL siRNA CANDIDATES

No.	Sense Strand	Antisense Strand
1	5' --ggauaccucucaacaauaca 3'	3' --uuccuaugggagaguuguuu--5'
2	5' --gcuccuuaccaacgaugaac 3'	3' --uucgaggaaugguugcuuacu--5'
3	5' --caaucugcuucguaguuuaga 3'	3' --gaguuaagacgaagcauuu--5'
4	5' --gucaugcguacgcgaaacu 3'	3'gccaguacagcaugcgcuuu--5

B. Zeta potential

Nanoparticle production was optimised to obtain a zeta potential of 89 mV, a mean particle size of 130 nm, and a polydispersity index of 0.516.

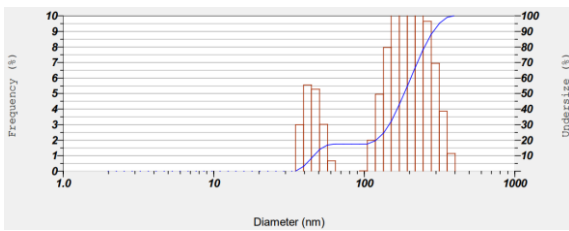


Fig. 4. Size distribution for optimised nanoparticles.

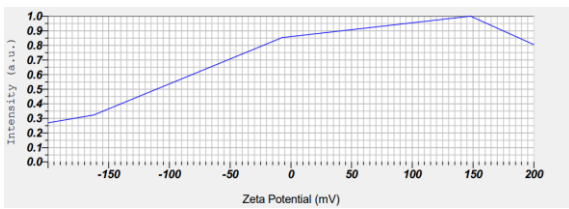


Fig. 5. Zeta potential distribution for optimised nanoparticles.

The optimised nanoformulation had a lower zeta potential of 35.8 mV, attributed to siRNA encapsulation. The particles also had an average particle size of 401.7 nm and a polydispersity index of 0.509.

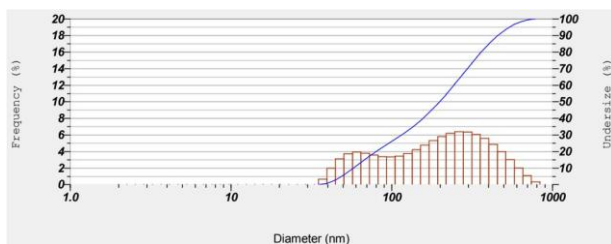


Fig. 6. Size distribution for siRNA nanoformulation.

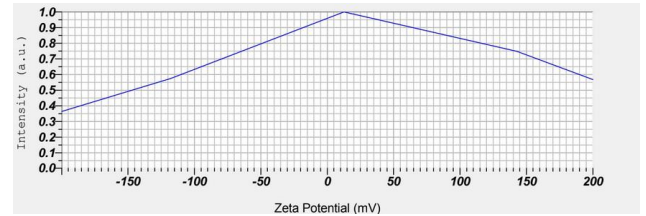


Fig. 7. Zeta potential distribution for siRNA nanoformulation.

C. SEM Analysis

1) *Newly Prepared Samples:* The chitosan nanoparticles and nanoformulation appeared as spherical beads in clusters at magnification higher than 100,000X. There was a variation in the shape and size due to the gap between their production and characterisation.

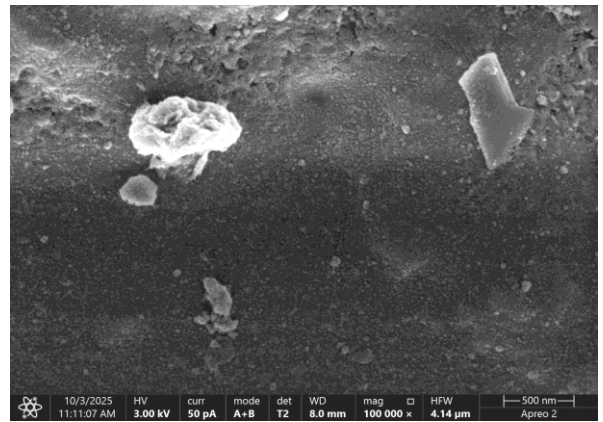


Fig. 8. Nanoformulation (prepared on 29th September) visualised at 100,000x magnification.

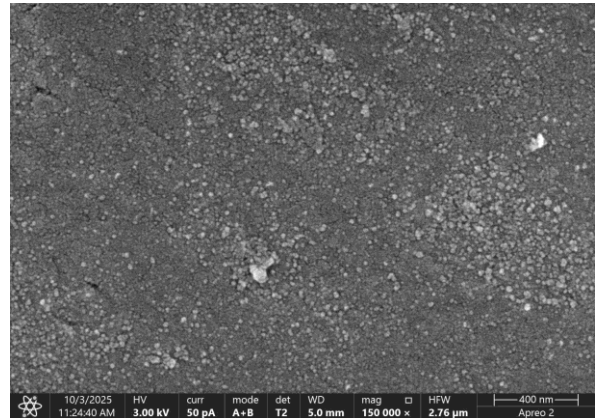


Fig. 9. Nanoformulation (prepared on 29th September) visualised at 150,000x magnification.

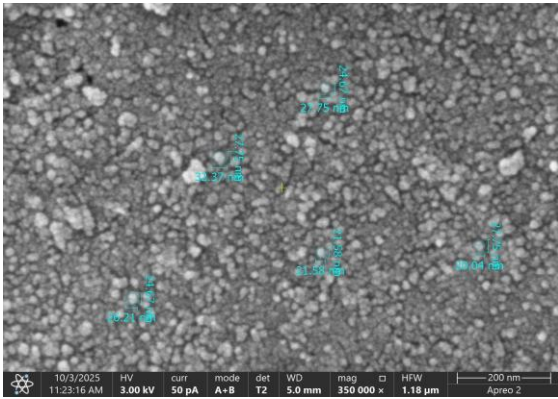


Fig. 10. Nanoformulation (prepared on 29th September) visualised at 350,000x magnification.

2) *3-Week-Old Samples*: The nanoparticles were uniformly dispersed, while the nanoformulation exhibited irregular surfaces, indicating successful encapsulation.

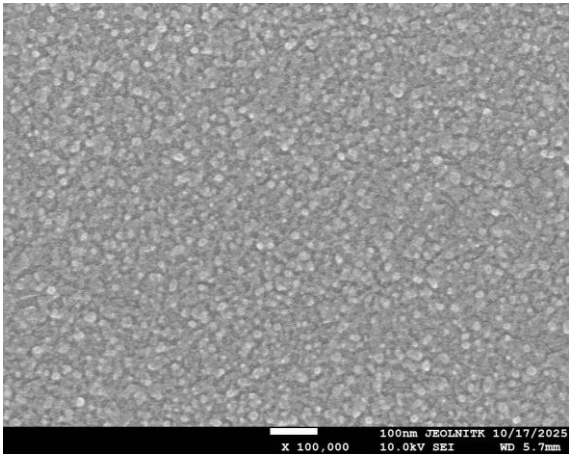


Fig. 11. 10 μL of chitosan nanoparticles visualised at 100,000x magnification.

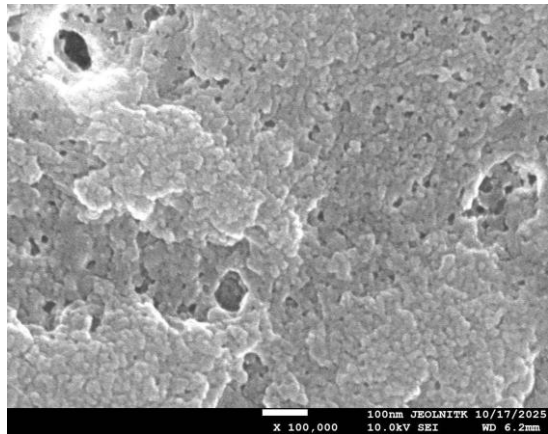


Fig. 12. 10 μL of nanoformulation (prepared on 29th September) visualised at 100,00x magnification.

D. Fluorescence microscopy

Fluorescent structures were clearly visible at 100x magnification and were comparable to the zoospores observed under phase contrast microscopy. This indicated successful internalisation of the siRNA into the zoospores

and their intended release from the nanoparticle complex.

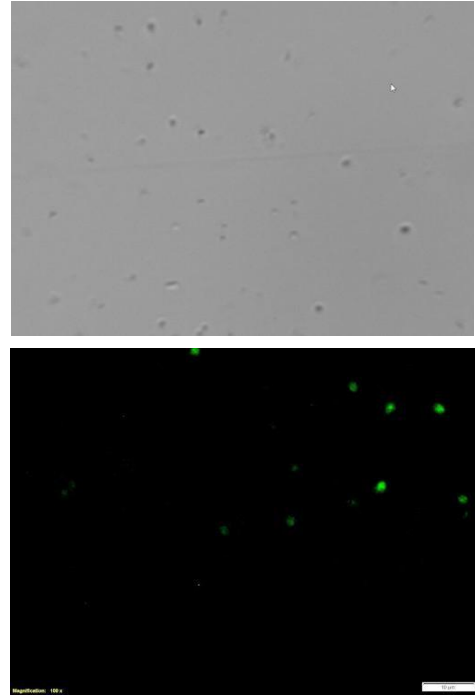


Fig. 13. Top - *P. capsici* zoospores visualised at 100x magnification using phase contrast microscopy. Bottom- Internalisation of the 6-FAM-tagged siRNA within *P. capsici* zoospores, visualised using fluorescence microscopy.

E. Zoospore Motility Assay

Motile zoospores were observed in the untreated, 1% acetic acid, and nanoparticle-treated samples. Zoospore samples that were treated with 7.23 μM siRNA, 100 μM siRNA, and the nanoformulation showed total reduction in zoospore motility, confirming the intended gene silencing.

F. Phytophthora capsici Culturing

A steady increase in growth was observed on carrot agar [17].

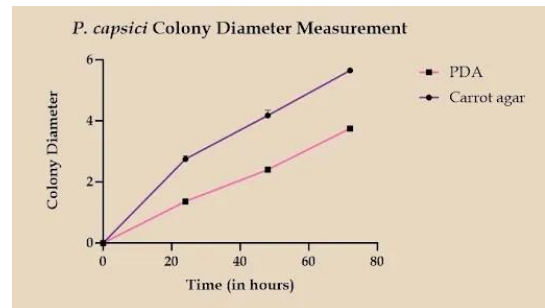


Fig. 14. Colony Diameter Measurement for *P. capsici* on PDA vs Carrot Agar.

G. Zoospore induction

Small globule-like cells were observed to be moving around.

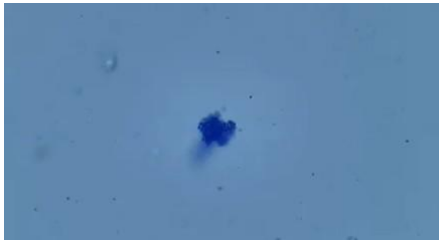


Fig. 15. *P. capsici* burst sporangium (dark blue), zoospores (small blue dots) stained in methylene blue under 40x.

H. Detached Leaf Assay

Lesion growth was measured across 72 hours to calculate the percentage inhibition as follows:

$$\text{Inhibition (\%)} = \frac{\text{Control lesion area} - \text{Sample lesion area}}{\text{Control lesion area}} \times 100$$

TABLE III. DETAILS OF THE SAMPLES USED

Sample	Preparation date	Polydispersity index	Hydrodynamic radius	Zeta Potential
Nanoparticle 1	4th September	0.454	95.1 nm	169.0 mV
Nanoparticle 2	6th September	0.488	267.5 nm	184.5 mV
Nanoparticle 3	10th September	0.516	130.1 nm	89.0 mV
Nanoformulation 1	27th September	2.318	6410.3 nm	-4.0 mV
Nanoformulation 2	29th September	0.509	401.7 nm	35.8 mV

1) Measuring the Efficacy of siRNA Treatments:

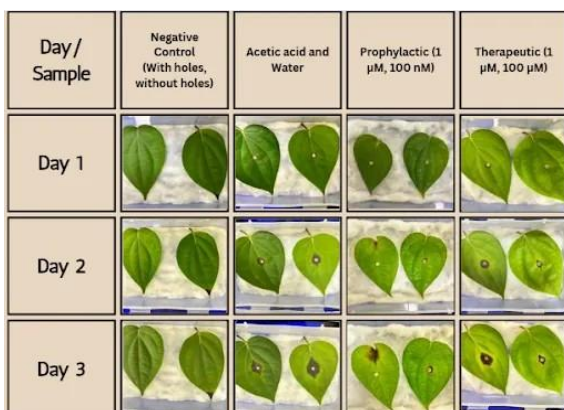


Fig. 16. Naked siRNA treatment on the leaves.

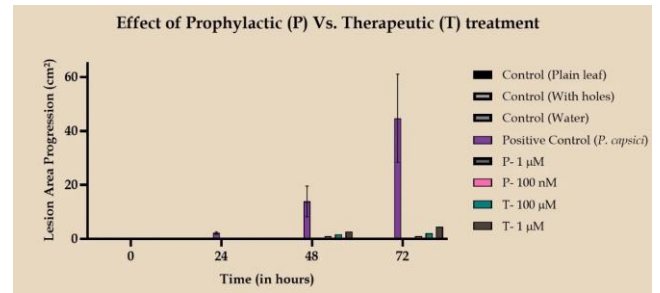


Fig. 17. Detached leaf assay: Effect of Prophylactic and therapeutic treatment with other controls.

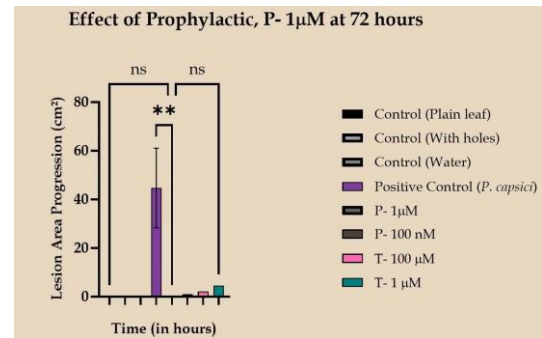


Fig. 18. 1-way ANOVA test on the effect of Prophylactic 1 μM siRNA among other controls at 72 hrs.

Prophylactic treatment of 1 μM and 100 nM siRNA showed 100% and 88.67% inhibition, respectively (the control lesion area was 8.74 cm²). Therapeutic treatment at 100 μM and 1 μM showed 76.08% and 48.52%, respectively. We can therefore infer that a 1 μM concentration of free siRNA is 100% effective when administered prophylactically.

2) Measuring the Efficacy of the Nanoformulation:

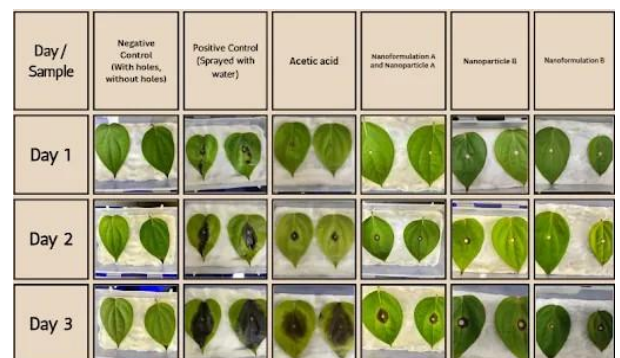


Fig. 19. Nanoformulation and nanoparticle treatment on leaves.

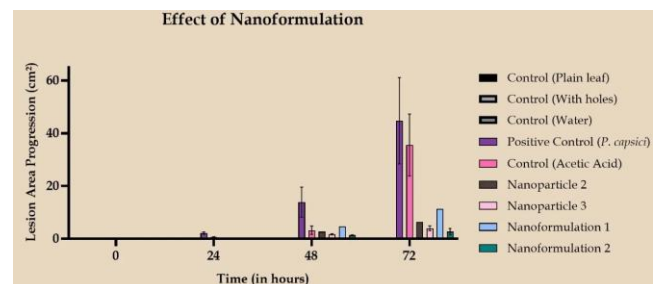


Fig. 20. Detached leaf assay: Effect of Nanoformulation among other controls.

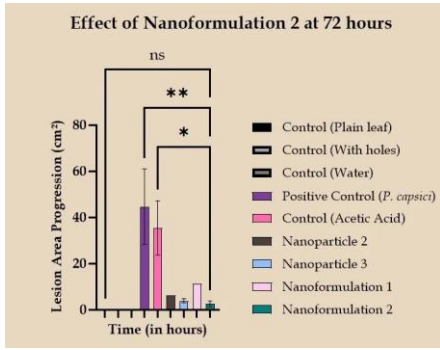


Fig. 21. 1-way ANOVA test on the effect of Nanoformulation 2 among other controls at 72 hrs.

Nanoformulation 2 showed a 93.977% inhibition of infection (control lesion area: 44.75 cm²).

3) Measuring the Efficacy of the Nanoformulation after 3 weeks:

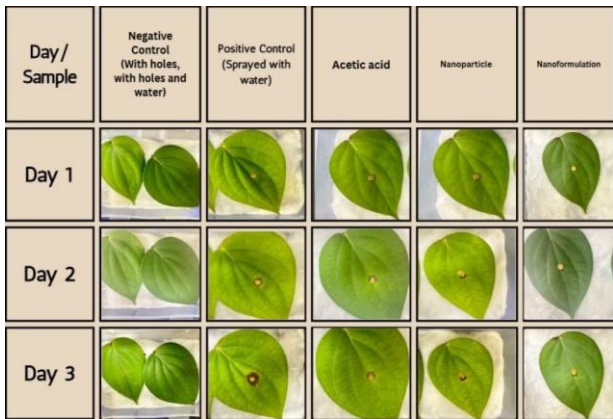


Fig. 22. Nanoformulation 2 and nanoparticle treatment on leaves after 3 weeks.

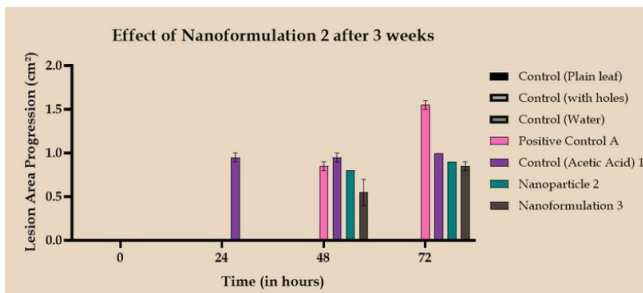


Fig. 23. Detached Leaf Assay: Effect of Nanoformulation 2 among other controls at 72 hrs after 3 weeks.

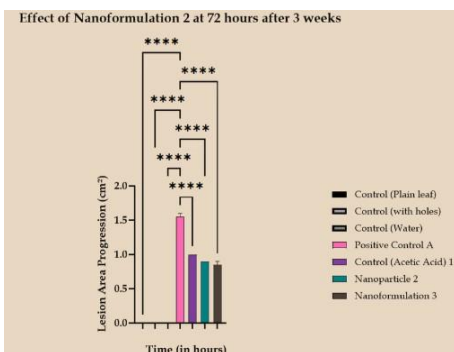


Fig. 24. 1-way ANOVA test on the effect of Nanoformulation 2 among other controls at 72 hrs after 3 weeks.

A 70% inhibition was observed upon treating leaves with a 3-week-old nanoformulation, representing a significant improvement over current biocontrol measures.

I. Detached Leaf Assay

100 nM siRNA appeared as a faint band (due to its low concentration). No bands were observed in the wells containing the nanoformulation, nanoformulation treated with RNase, and the nanoparticle. Successful encapsulation was inferred from the entrapment of siRNA in the well.

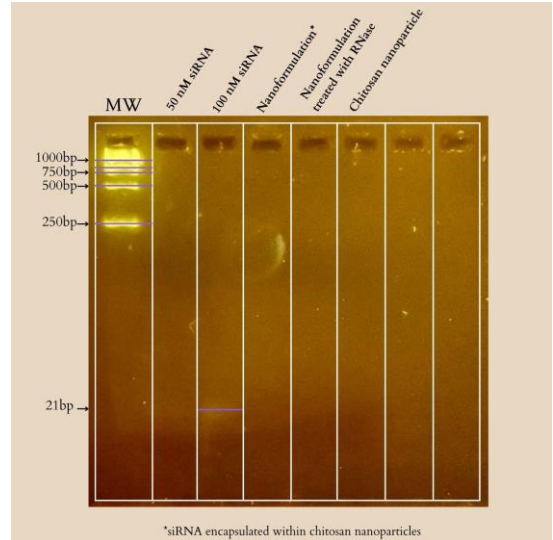


Fig. 25. Visualisation of the gel under a UV transilluminator.

J. Entrapment Efficiency

The concentration of siRNA in the supernatant (from a 20.778 µg/mL nanoformulation sample) was 2.2 µg/mL. These values produced an entrapment efficiency of 89.41%, indicating effective encapsulation [16].

IV. SOFTWARE

A. Approach

While siRNA-nanoparticle (siRNA-NP) formulations offer a promising approach to tackling plant pathogens, finding the ideal siRNA-nanoparticle combination is challenging. To address these hurdles, a two-module software was developed to rapidly and reproducibly produce siRNA-nanoparticle gene silencing systems.

The first component, siUltimate, integrates several existing siRNA design platforms, including siDirect, siRNAPred, and DuplexFold [18],[19]. Selenium, a Python web scraping framework was used for this purpose, as the websites lacked APIs but were simple and easy to navigate. The Machine Learning model, S.E.N.S.E., was trained on molecular descriptors evaluated from siRNA-NP complexes using docking and molecular dynamics simulations.

Developing the model consisted of selecting relevant features, applying standard scaling, and removing outliers. The model was trained using the XGBoost algorithm to

predict the target variable ‘Ligand RMSD’. 217 features were generated as follows:

1) *One-hot encoded sequences (215 features)*: Each siRNA sequence (up to 43 nucleotides, including guide and passenger strands) is represented using one-hot encoding. For each position, five binary variables indicate whether the nucleotide is A, U, G, C, or empty.

2) *Sequence composition features (18 features)*:

GC content: Measures the percentage of G and C nucleotides.

AU content: Measures the percentage of A and U nucleotides.

Dinucleotide counts: 16 features account for the frequency of adjacent nucleotide pairs.

Sequence entropy: Captures the variation, frequency, and positions of codons or bases in an input siRNA sequence [20].

3) *Nanoparticle type (2 features)*: The model assigned two binary variables (0 or 1) to indicate the presence of chitosan or lipid nanoparticles.

Total: $215 + 1 + 1 + 16 + 1 + 2 = 236$ features (the number 217 suggests features were removed during preprocessing, possibly redundant padding positions) [21].

C. Software Results

An RMSE of 33.30 and an R-squared of 0.7459 were obtained, indicating that the model explained approximately 75% of the variance in the docking scores [22].

It was also observed that chitosan nanoparticles scored 68.4 points higher than lipid nanoparticles, likely due to differences in surface chemistry and charge. AU content came in second with a coefficient of 37.1, followed by GC content at 31.0, and CG dinucleotide frequency at 1.5.

TABLE IV. THE ERROR CALCULATION WITH THE DOCKING SCORES PERFORMED THROUGH HDock AND THE PREDICTED SCORES OF OUR MODEL

Seq No	Duplex Sequence (5'→3' / 5'→3')	Docking Score (Chitosan)	Docking Score (Lipid)	Error Calc (Chitosan)	Error Calc (Lipid)
1	GGUACUACAACUAGUGUGACU UCACACUAGUUGUAGUACCAG	-215.51	-114.75	+36	-20
2	CAGAGCUGAAGGAUAUGAAGA UUCAUAUCCUUCAGCUCUGUG	-246.64	-137.74	+11	-4
3	GGAGACAGCGACAAGUUGUCG ACAACUUGUCGUCUCUCCAA	-215.24	-106.34	+39	-31
4	CCCGAGUGCGGUUCACUAGG UAGUGAAACCGCACUCGGGUG	-292.31	-158.95	-38	+21
5	GGGAGAGACUGGUGAUGAAGG UUCAUCACCGACUCUCCCC	-281.82	-151.31	-27	+14

V. BIOSECURITY

A. Biosafety

Risks associated with the project were assessed in accordance with the World Health Organisation's definition of Dual Use Research of Concern (DURC). siRNA can be modified to target other *P. capsici* genes or agricultural pathogens. However, the approach can also be misused to target key plant genes that could negatively impact the agriculture industry. To minimise the risk of off-target effects, NCBI BLAST and GESS analysis were performed. Chitosan nanoparticles offer an environmentally safe carrier system, as they are biodegradable into non-toxic

products [23]-[26].

B. Lab safety

All experimental work was conducted in compliance with institutional and national biosafety guidelines. All experiments were performed in a Biosafety Level-2 (BSL-2) laboratory equipped with a Class-2 Biosafety cabinet. All work involving *P. capsici* was carried out under aseptic conditions with the appropriate PPE. Biological and chemical wastes were segregated, decontaminated, and disposed of in accordance with institutional safety protocols. Lab personnel were trained in standard molecular techniques, equipment handling, and risk assessment to ensure the safe execution of the project.

VI. HUMAN-CENTERED DESIGN

The project was driven by the goal of creating a solution that is practical, scalable, and easy for the farmers to use. Conversations with farmers and agricultural experts, along with visits to pepper plantations across South India, revealed the limitations of chemical fungicides and the need for sustainable alternatives. These insights led to a simple implementation strategy: the nanoformulation is lyophilised using a cryoprotectant such as sucrose to produce a stable, solid product that can be stored at room temperature, eliminating cold-chain requirements and enabling easy field use through simple resuspension in water. In parallel, outreach efforts engaged the broader community through visits to over 20 schools, reaching approximately 3000 individuals and building awareness of synthetic biology, plant pathogens, and the potential of siRNA-based solutions.

VI. CONCLUSION

This study establishes an effective RNAi-based biocontrol strategy for controlling *Phytophthora capsici* infection in black pepper (*Piper nigrum*), integrating target gene selection, computational siRNA design, and a chitosan nanoparticle delivery system. The transcription factor *bZIP1* was identified as a key regulator of pathogenicity and has proven to be an effective molecular target. The siRNA was successfully encapsulated in chitosan nanoparticles, yielding stable nanoformulations with efficient cellular uptake and gene-silencing activity, validated by the experimental framework.

Biological assays confirmed significant inhibition of zoospore motility and strong disease suppression. The nanoformulation outperformed free siRNA and retained efficacy even after prolonged storage. The use of biodegradable chitosan and strict biosafety practices ensures the environmental safety and sustainability that we aim to achieve.

siUltimate is a pipeline that streamlines siRNA design while accounting for off-target effects and secondary structure stability. S.E.N.S.E., is a Machine Learning model that predicts siRNA–nanoparticle stability using data from docking and molecular dynamics simulations. Together, these tools transform a process that previously took weeks into a rapid, reliable workflow that can be completed within minutes.

REFERENCES

- [1] L. D. Thao et al., “Current species of oomycetes associated with foot rot disease of black pepper in Vietnam,” *Tropical Plant Pathology*, vol. 49, no. 5, pp. 633–648, Jun. 2024, doi: <https://10.1007/s40858-024-00662-4>.
- [2] M. Jibat and M. Asfaw, “Management of foot rot (*Phytophthora capsici*) disease of black pepper (*Piper nigrum* L.) through fungicides and cultural practices in Southwestern Ethiopia,” *International Journal of Agricultural Research Innovation and Technology*, vol. 13, no. 1, pp. 48–50, Aug. 2023, doi: <https://10.3329/ijarit.v13i1.67973>.
- [3] V.L.Nguyen, “Spread of *Phytophthora capsici* in Black Pepper (*Piper nigrum*) in Vietnam,” *Engineering*, vol. 07, no. 08, pp. 506–513, Jan. 2015, doi: <https://10.4236/eng.2015.78047>.
- [4] P. T. Sreethu, M. M. Paul, P. P. Gopinath, I. L. Shahana, and N. S. Radhika, “Foliar symptom-based disease detection in black pepper using a convolutional neural network,” *Phytopathology Research*, vol. 7, no. 1, Mar. 2025, doi: <https://10.1186/s42483-024-00305-1>.
- [5] S. Bhat, V. Arunachalam, V. Paramesha, and N. Gaonkar, “Quantifying the economic impact and management strategies for foot rot (*Phytophthora capsici* L.) disease on black pepper cultivation in West Coast India: Farm-level insights,” *Plant Science Today*, Feb. 2025, doi: <https://doi.org/10.14719/pst.6764>.
- [6] K. H. Lamour, R. Stam, J. Jupe, and E. Huitema, “The oomycete broad-host-range pathogen *Phytophthora capsici*,” *Molecular Plant Pathology*, vol. 13, no. 4, pp. 329–337, Oct. 2011, doi: <https://10.1111/j.1364-3703.2011.00754.x>.
- [7] Blanco, F. A., & Judelson, H. S. (2005). A bZIP transcription factor from *Phytophthora* interacts with a protein kinase and is required for zoospore motility and plant infection. *Molecular Microbiology*, 56(3), 638–648. <https://doi.org/10.1111/j.1365-2958.2005.04575.x>
- [8] K. H. Lamour et al., “Genome Sequencing and Mapping Reveal Loss of Heterozygosity as a Mechanism for Rapid Adaptation in the Vegetable Pathogen *Phytophthora capsici*,” *Molecular Plant-Microbe Interactions*, vol. 25, no. 10, pp. 1350–1360, oct. 2012, doi: <https://doi.org/10.1094/mpmi-02-12-0028-r>.
- [9] S. Vijayakumar, G. G. Saraswathy, and M. Sakuntala, “Transcriptomic analysis reveals pathogenicity mechanisms of *Phytophthora capsici* in black pepper,” *Frontiers in Microbiology*, vol. 15, Nov. 2024, doi: <https://doi.org/10.3389/fmicb.2024.1418816>.
- [10] I. V. Grigoriev et al., “PhycoCosm, a comparative algal genomics resource,” *Nucleic Acids Research*, vol. 49, no. D1, pp. D1004–D1011, Oct. 2020, doi: <https://doi.org/10.1093/nar/gkaa898>.

- [11] Y. Naito, T. Yamada, K. Ui-Tei, S. Morishita, and K. Saigo, "siDirect: highly effective, target-specific siRNA design software for mammalian RNA interference," *Nucleic Acids Research*, vol. 32, no. Web Server, pp. W124–W129, Jul. 2004, doi: <https://doi.org/10.1093/nar/gkh442>.
- [12] D. H. Mathews, M. D. Disney, J. L. Childs, S. J. Schroeder, M. Zuker, and D. H. Turner, "Incorporating chemical modification constraints into a dynamic programming algorithm for prediction of RNA secondary structure," *Proceedings of the National Academy of Sciences*, vol. 101, no. 19, pp. 7287–7292, May 2004, doi: <https://doi.org/10.1073/pnas.0401799101>.
- [13] A. R. Gruber, R. Lorenz, S. H. Bernhart, R. Neubock, and I. L. Hofacker, "The Vienna RNA Websuite," *Nucleic Acids Research*, vol. 36, no. Web Server, pp. W70–W74, May 2008, doi: <https://doi.org/10.1093/nar/gkn188>.
- [14] G. Schramm and R. Ramey, "siRNA design including secondary structure target site prediction," *Nature Methods*, vol. 2, no. 8, pp. 632–632, Aug. 2005, doi: <https://doi.org/10.1038/nmeth780>.
- [15] B. S. E. Heale, "siRNA target site secondary structure predictions using local stable substructures," *Nucleic Acids Research*, vol. 33, no. 3, pp. e30–e30, Feb. 2005, doi: <https://doi.org/10.1093/nar/gni026>.
- [16] Katas, H., & Alpar, H. O. (2006c). Development and characterisation of chitosan nanoparticles for siRNA delivery. *Journal of Controlled Release*, 115(2), 216–225. <https://doi.org/10.1016/j.jconrel.2006.07.021>
- [17] Chemeltorit, P.P., Mutaqin, K.H. & Widodo, W. Combining *Trichoderma hamatum* THSW13 and *Pseudomonas aeruginosa* BJ10–86: a synergistic chilli pepper seed treatment for *Phytophthora capsici* infested soil. *Eur J Plant Pathol* 147, 157–166 (2017). <https://doi.org/10.1007/s10658-016-0988-5>
- [18] M. Amarzguioui and H. Prydz, "An algorithm for selection of functional siRNA sequences," *Biochemical and Biophysical Research Communications*, vol. 316, no. 4, pp. 1050–1058, Apr. 2004, <https://doi.org/10.1016/j.bbrc.2004.02.157>.
- [19] K. Ui-Tei et al., "Guidelines for the selection of highly effective siRNA sequences for mammalian and chick RNA interference," *Nucleic Acids Research*, vol. 32, no. 3, pp. 936–948, 2004, doi: <https://doi.org/10.1093/nar/gkh247>.
- [20] P. C. Patel, L. Hao, W. S. Au Yeung, and C. A. Mirkin, "Duplex End Breathing Determines Serum Stability and Intracellular Potency of siRNA–Au NPs," *Molecular Pharmaceutics*, vol. 8, no. 4, pp. 1285–1291, Jun. 2011, doi: <https://doi.org/10.1021/mp200084v>.
- [21] S. N. Barnaby, A. Lee, and C. A. Mirkin, "Probing the inherent stability of siRNA immobilised on nanoparticle constructs," *Proceedings of the National Academy of Sciences of the United States of America*, vol. 111, no. 27, pp. 9739–9744, Jun. 2014, doi: <https://doi.org/10.1073/pnas.1409431111>.
- [22] A. Reynolds, D. Leake, Q. Boese, S. Scaringe, W. S. Marshall, and A. Khvorova, "Rational siRNA design for RNA interference," *Nature Biotechnology*, vol. 22, no. 3, pp. 326–330, Feb. 2004, doi: <https://doi.org/10.1038/nbt936>.
- [23] A. Oberlintner, M. Bajić, G. Kalčíková, B. Likozar, and U. Novak, "Biodegradability study of active chitosan biopolymer films enriched with Quercus polyphenol extract in different soil types," *Environmental Technology & Innovation*, vol. 21, p. 101318, Dec. 2020, doi: <https://10.1016/j.eti.2020.101318>
- [24] B. Bhuvanachandra et al., "New Class of Chitosanase from *Bacillus amyloliquefaciens* for the Generation of Chitooligosaccharides," *Journal of Agricultural and Food Chemistry*, vol. 69, no. 1, pp. 78–87, Jan. 2021, doi: <https://10.1021/acs.jafc.0c05078>
- [25] G. Ali, M. Sharma, E.-S. Salama, Z. Ling, and X. Li, "Applications of chitin and chitosan as natural biopolymers: potential sources, pretreatments, and degradation pathways," *Biomass Conversion and Biorefinery*, vol. 14, no. 4, pp. 4567–4581, Apr. 2022, doi: <https://10.1007/s13399-022-02684-x>.
- [26] N. Thadathil and S. P. Velappan, "Recent developments in chitosanase research and its biotechnological applications: A review," *Food Chemistry*, vol. 150, pp. 392–399, Oct. 2013, doi: <https://10.1016/j.foodchem.2013.10.083>.